

Alignment of Palladium Complexes into Columnar Liquid Crystals Driven by Peripheral Triphenylene Substituents

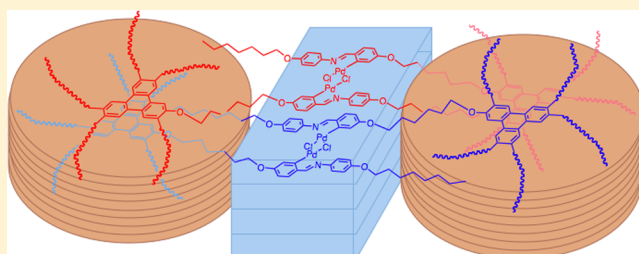
Emiliano Tritto,[†] Rubén Chico,[†] Gerardo Sanz-Enguita,[‡] César L. Folcia,[§] Josu Ortega,[‡] Silverio Coco,^{*,†} and Pablo Espinet^{*,†}

[†]IU CINQUIMA/Química Inorgánica, Facultad de Ciencias, Universidad de Valladolid, 47071 Valladolid, Castilla y León, Spain

[‡]Department of Applied Physics II and [§]Department of Condensed Matter Physics, University of the Basque Country, UPV/EHU, 48080 Bilbao, Spain

S Supporting Information

ABSTRACT: A new triphenylene-imine (ImH) and its ortho-palladated complexes ($\mu\text{-X})_2[\text{Pd}_2\text{Im}_2]$ ($\text{X} = \text{CH}_3\text{COO}^-$, Cl^- , Br^-), ($\mu\text{-Cl})(\mu\text{-SC}_n\text{H}_{2n+1})[\text{Pd}_2\text{Im}_2]$ ($n = 6, 12$), $[\text{PdIm}(\text{acac})]$ $[\text{PdImCl}(\text{CNC}_6\text{H}_4\text{OC}_{12}\text{H}_{25})]$, $[\text{PdImCl}(\text{CNC}_6\text{H}_3(\text{OC}_{12}\text{H}_{25})_2)]$, and $[\text{PdImCl}(\text{CNC}_6\text{H}_2(\text{OC}_{12}\text{H}_{25})_3)]$ have been prepared. The free imine ligand is not a liquid crystal, but most ortho-metalated dinuclear palladium complexes and the mononuclear trialkoxyphenyl isocyanide derivative display columnar mesophases at temperatures close to ambient. For the dimeric complexes the mesophase obtained is always columnar rectangular (Col_r), with an uncommon structure: the dimeric triphenylene-Pd complex-triphenylene molecules give rise to a triple-column stacking consisting of two columns of stacked triphenylene groups connected to a central column formed by stacking of two ortho-palladated dimeric moieties. For the trialkoxyphenyl isocyanide derivative a related polymer-like arrangement of columns alternating stacking of triphenylenes with stacking of two ortho-palladated dimeric moieties is found. The mesophase structure is columnar oblique (Col_{ob}). The free imine and all palladium complexes exhibit fluorescence at room temperature in dichloromethane solution, associated with the triphenylene core.



INTRODUCTION

Columnar liquid crystals have received considerable attention in recent years as functional materials for application in nanoscale conductive devices, field-effect transistors, or photovoltaic solar cells.^{1,2} Many systematic studies on the influence of the molecular constitution and stacking on the mesomorphism have been reported, mostly on conventional organic liquid crystals.^{1d,3} However, the number of studies on metal-containing liquid crystals (metallomesogens) is comparatively lower.^{4,5}

We have recently reported columnar hexagonal metallomesogens based on supramolecular complexes formed from metallo-organic acids hydrogen bonded to a substituted triazine as proton acceptor. The metal fragments are dangling around the central columnar triazine stacking.⁶ They are interesting soft materials formally reminiscent of a polymeric backbone (the column) supporting the organometallic fragments. However, both the formation of the column and its connection to the fragments are reversible upon heating or by dissolution. This synthetic approach permits linking different metallic fragments to the column. New or modified properties might appear in the aggregate depending on the distribution of the metal fragments: for instance, helical structures, interfragment interactions in the columnar aggregate (e.g., metal-metal interactions along the columnar direction), or properties associated with metal-metal bonds (e.g., luminescence or electric one-dimensional conductivity along the piled metal fragments).

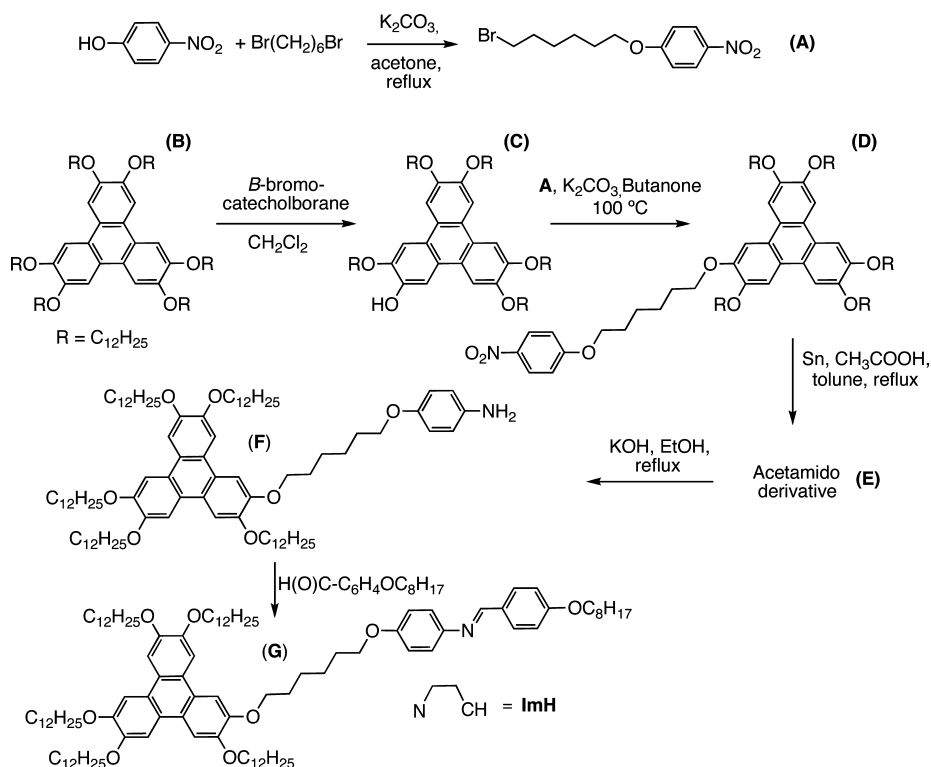
The utility of these systems could be limited by their relatively low thermal stability because of the lability of the hydrogen bond. Therefore, we decided to develop related systems based on simpler and more robust molecules. The triphenylene moiety looked like a good choice because it is a stable classical organic system with many available procedures to modify and connect different groups to the triphenylene core. This group is used often to induce columnar mesophases in organic liquid crystals,^{1d,3} and it is found also in a few nonconventional organic liquid crystals arising from the chemical linkage of disc-like triphenylenes and rod-shaped moieties,⁷ where phases other than columnar can also arise. In addition, there have already been a few reports of liquid crystalline metal-organic triphenylene systems with covalently bonded Hg,⁸ Cr,⁹ Zn,¹⁰ Cu,¹¹ and Ni^{II} and Ag^I complexes.¹²

With these precedents we considered that ortho-palladated complexes (one of the most studied families in the field of metallomesogens) should be easy to attach to the triphenylene columnar core and would display good thermal stability.⁴ We have obtained a family of interesting liquid crystalline mono- and dinuclear ortho-metalated palladium complexes that display unusual columnar mesophases close to ambient temperature. Their structure contains a triple stack of a central column of pairs

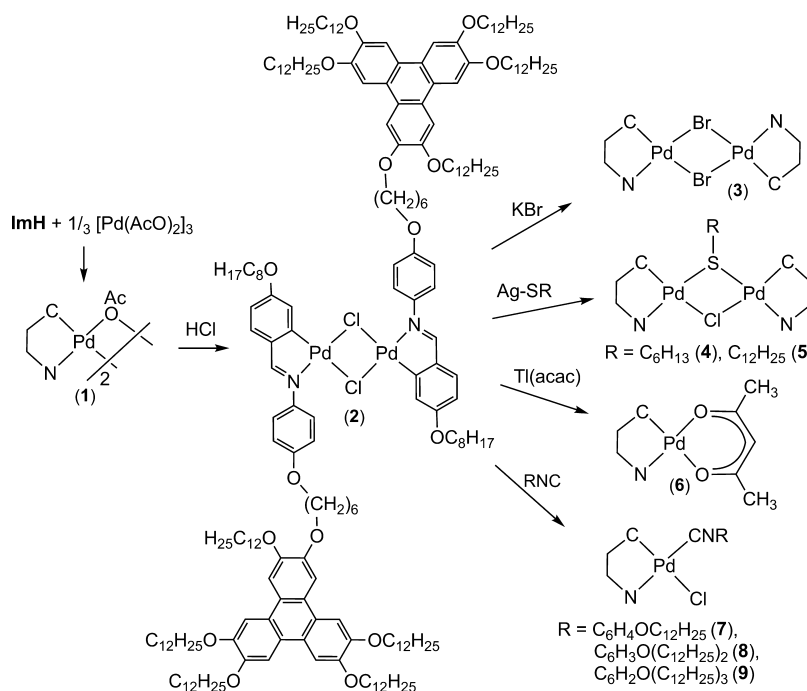
Received: November 20, 2013

Published: March 17, 2014

Scheme 1. Synthesis of 2-(6-(4-Aminophenoxy)hexyloxy)-3,6,7,10,11-pentakis(dodecyloxy)triphenylene and the Imine Ligand



Scheme 2. Synthesis of Palladium Ortho-Metalated Complexes



of ortho-palladated dimeric moieties, flanked by two columns of triphenylene groups connected to it.

RESULTS AND DISCUSSION

Synthesis and Characterization. The Schiff base ImH was synthesized by conventional methods as shown in Scheme 1.^{13,14} Details are given in the Supporting Information.

The cyclopalladated complexes were synthesized as depicted in Scheme 2. Elemental analyses, yields, relevant IR data, and ¹H NMR spectra for the complexes are given in the Supporting Information. The ¹H NMR resonances associated with the ortho-palladated imine moiety support the isomeric purity of the complexes. The ortho metalation of the imine ligand to give the acetato complex 1 was carried out as described elsewhere.¹⁵ The typical structural features of complexes analogous to 1–3, but

without a triphenylene group, have been reported in detail in previous papers.¹⁶ The acetato-bridged complexes are butterfly-shaped at the Pd core, while the halogen-bridged complexes are planar. In these dimers only the isomer with an *anti* arrangement of the two imine fragments is detected by ¹H NMR.

For the thiolato-bridged complex, a *syn* arrangement of the imine moieties with the thiolato group *trans* to the imine nitrogen atoms is proposed, as found in analogous palladium complexes.¹⁷ The mononuclear species 6–9 show ¹H NMR spectra very similar to those of the dinuclear complexes, in addition to the corresponding signals of the introduced ligand. Thus, for the acetylacetonato (acac) complexes a singlet at ca. 5.4 ppm (acac CH group) and two singlets at 2.1 and 1.9 ppm (acac nonequivalent Me groups) are observed.

The isonitrile derivatives display the signals of the substituted aromatic ring and the signals corresponding to the respective chains. A ROESY-1D (monodimensional rotating frame Overhauser effect spectroscopy) experiment on compound 9 showed an ROE effect on the H signal of the imine ring upon irradiation of the singlet of the aromatic ring of the isonitrile, supporting a *trans* disposition of the isonitrile with respect to the imine nitrogen.

Mesomorphic Behavior. The free imine ligand used is not mesogenic, but all of the dinuclear palladium complexes show mesomorphic behavior, except for the acetato complex (usually butterfly-shaped ortho-metalated acetato-bridged complexes are not mesomorphic because of their unfavorable molecular shape).^{4b,16d} In contrast, the mononuclear derivatives do not show liquid crystal behavior, except for the trialkoxyphenyl isocyanide complex. Optical, thermal, and thermodynamic data of the compounds, obtained by polarized optical microscopy (POM), differential scanning calorimetry (DSC), and X-ray scattering, are collected in Table 1.

In the five compounds that exhibit mesomorphic behavior only one liquid crystalline phase is observed between the isotropic state and the low-temperature crystal. The first DSC

heating scan of all complexes shows the corresponding melting and clearing transitions. However, in the cooling cycle no sign of crystallization or glass transition was detected; the sample simply becomes less fluid and looks frozen, suggesting that an undetectable transformation to a glassy state has occurred. In some compounds, unusually small enthalpy values were detected for crystallization upon cooling and for the corresponding melting transition in the second heating scan. This unusually small enthalpy value is likely due to only partial crystallinity of the sample, which is a frequent behavior in this type of system. It is important to note that the melting and clearing points appear in the DSC scans as broad transitions (Figures S1–S3, Supporting Information). For this reason the significance and accuracy of these data are probably low. The POM optical texture, when formed on cooling from the isotropic melt, shows a mosaic texture (Figure 1), which suggests a columnar mesophase, later identified as Col_r for complexes 2–5 and Col_{ob} for complex 9.

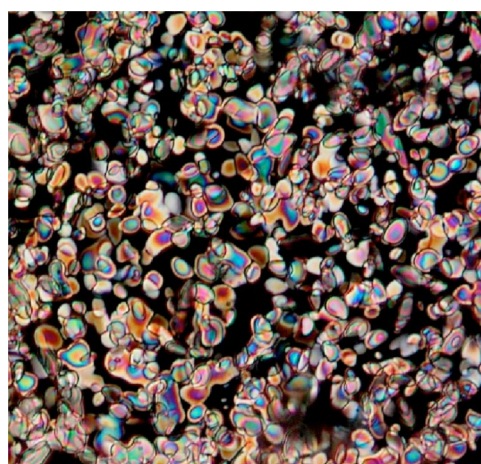


Figure 1. POM texture ($\times 100$) of the mesophase of $(\mu\text{-SC}_6\text{H}_{13})(\mu\text{-Cl})[\text{Pd}_2\text{Im}_2]$ (compound 4) (chosen as a representative example, see Figure S4 in the Supporting Information for more POM textures) near the clearing point obtained on cooling. In the figure liquid crystalline domains coexist with the isotropic state.

Table 1. Optical, Thermal, and Thermodynamic Data of Ortho-Palladated Imine Complexes

compound	transition ^a	temp ^b (°C)	ΔH^b (kJ mol ⁻¹)
imine (ImH)	C \rightarrow C'	35	27.70
	C \rightarrow I	43	31.71
$(\mu\text{-OAc})_2[\text{Pd}_2\text{Im}_2]$ (1)	C \rightarrow I ^c	36	72.69
$(\mu\text{-Cl})_2[\text{Pd}_2\text{Im}_2]$ (2)	C \rightarrow Col _r	34	1.56
	Col _r \rightarrow I	56	1.44
$(\mu\text{-Br})_2[\text{Pd}_2\text{Im}_2]$ (3)	C \rightarrow Col _r	32	4.79 ^d
	Col _r \rightarrow I	51	8.20
$(\mu\text{-Cl})(\mu\text{-SC}_6\text{H}_{13})[\text{Pd}_2\text{Im}_2]$ (4)	Col _r \rightarrow I	76	5.34
$(\mu\text{-Cl})(\mu\text{-SC}_{12}\text{H}_{25})[\text{Pd}_2\text{Im}_2]$ (5)	C \rightarrow Col _r	36	2.86
	Col _r \rightarrow I	66	1.34
$[\text{PdIm}(\text{acac})]$ (6)	C \rightarrow I	35	38.9
$[\text{PdImCl}(\text{CNC}_6\text{H}_4\text{OC}_{12}\text{H}_{25})]$ (7)	C \rightarrow I	32	16.9
$[\text{PdImCl}(\text{CNC}_6\text{H}_3(\text{OC}_{12}\text{H}_{25})_2)]$ (8)	C \rightarrow I	30	12.1
$[\text{PdImCl}(\text{CNC}_6\text{H}_2(\text{OC}_{12}\text{H}_{25})_3)]$ (9)	C \rightarrow Col _{ob}	28	2.05
	Col _{ob} \rightarrow I	74	0.53

^aAbbreviations: Col_r, columnar rectangular; Col_{ob}, columnar oblique; I, isotropic liquid; C and C', crystals. ^bData collected from the second heating DSC cycle. The transition temperatures are given as peak onsets. ^cData from the first heating scan. ^dCombined transition.

The mesomorphic behaviors of the complexes with halogen bridges (2 and 3) are very alike. The transition temperatures are slightly lower for the bromo derivative, probably due to the larger size of the bromo in comparison to the chloro ligand. For the mixed chloro–thiolate derivatives (4 and 5), the introduction of the additional chain of the thiolate group leads, as expected, to an interesting decrease in melting temperatures. This decrease is generally more pronounced as the length of the chain increases, as observed here. For the mononuclear complexes, only the trialkoxyphenyl isocyanide complex (9) displays liquid crystal properties. The presence of the three additional alkoxy chains in the molecule, which will certainly contribute to fill up a discotic shape, must be the reason for this behavior.

In order to elucidate the structural properties of these mesophases, X-ray diffraction measurements were carried out. In all cases the diffraction diagram is typical of a liquid crystal phase: a diffuse halo at wide angles, indicating the fluid character of the phase, and a set of sharp peaks in the small-angle region (see Figures 2 and 3 and Figures S5–S7 (Supporting Information)). The peak positions of the different materials under study are summarized in Table 2 together with their relative intensities. In the case of compounds 2 and 3, the X-ray diagram could be compatible with a simple lamellar structure,

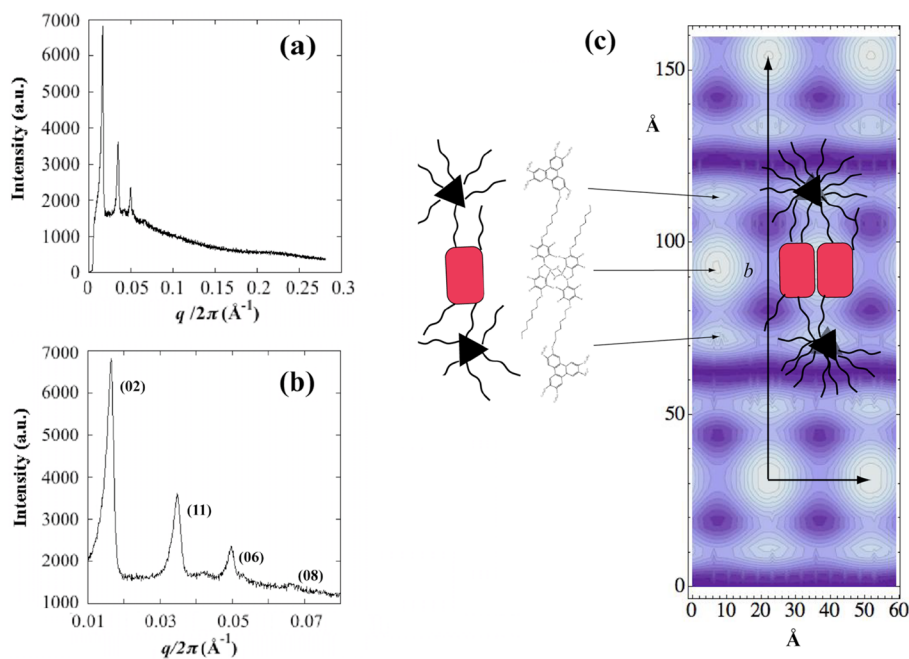


Figure 2. (a) X-ray diagram of compound **2** at 43 °C. q is the diffraction vector. (b) Detail of the small-angle region. In the figure the Miller indices of the different peaks are indicated. (c) Corresponding charge-density map. The electron density distribution is compared to the molecular structure. Both images are depicted at the same scale. In the figure the proposed model for the molecular packing is also schematized.

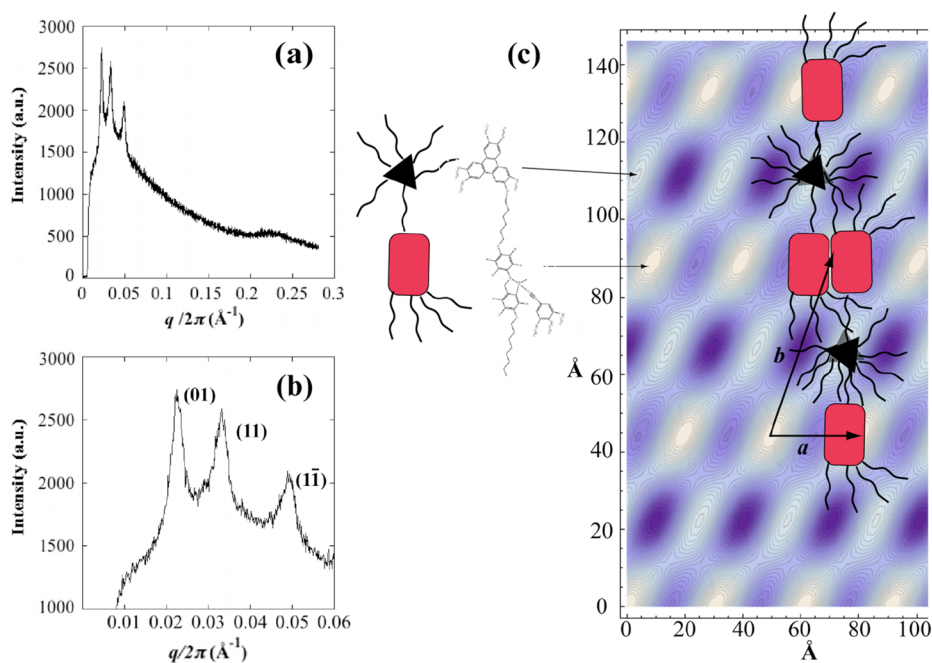


Figure 3. (a) X-ray diagram of compound **9** at 45 °C. q is the diffraction vector. (b) Detail of the small-angle region. In the figure the Miller indices of the different peaks are indicated. (c) Corresponding charge-density map. The electron density distribution is compared to the molecular structure. Both images are depicted at the same scale. In the figure the scheme of the molecular packing is also represented.

assuming a certain degree of laxity in the angular position of the second peak. However, this simple scheme of indexation is clearly not applicable to the similar compounds **4** and **5**. Consequently, a 2D translation lattice is considered for all the dinuclear materials (compounds **2–5**). On the other hand, it is important to note that the diffraction diagrams show a set of reflections that correspond to different harmonics of a given periodicity together with another peak that represents a different periodicity, as can be deduced from Table 2. As a consequence,

the unit cell is not univocally determined. In view of this, it is clear that some extra criterion is required to model the structures. Therefore, we have indexed the X-ray diagrams assuming the symmetry as high as possible, provided that suitable packing conditions are fulfilled. Our strategy consisted of the construction of electron density maps (Fourier maps) using the diffracted intensities after selecting a given unit cell. These maps allow us to obtain an image of the structure by positioning the molecules in the unit cell.

Table 2. Summary of the X-ray Scattering Results^a

compound	temp (°C)	cell param	peak position $q/2\pi$ (Å ⁻¹)/normalized intensity	Miller index
$(\mu\text{-Cl})_2[\text{Pd}_2\text{Im}_2]$ (2)	43	$a = 29.6 \text{ \AA}$ $b = 122.7 \text{ \AA}$	0.0163/1	(02)
			0.0347/0.383	(11)
			0.0497/0.175	(06)
			0.0666/0.0189	(08)
$(\mu\text{-Br})_2[\text{Pd}_2\text{Im}_2]$ (3)	45	$a = 29.45 \text{ \AA}$ $b = 117.6 \text{ \AA}$	0.017/1	(02)
			0.035/0.363	(11)
			0.0514/0.400	(06)
			0.068/0.045	(08)
$(\mu\text{-Cl})(\mu\text{-SC}_6\text{H}_{13})[\text{Pd}_2\text{Im}_2]$ (4)	50	$a = 26.1 \text{ \AA}$ $b = 125.0 \text{ \AA}$	0.016/1	(02)
			0.0320/0.016	(04)
			0.0392/0.390	(11)
			0.048/0.230	(06)
			0.0641/0.011	(08)
$(\mu\text{-Cl})(\mu\text{-SC}_{12}\text{H}_{25})[\text{Pd}_2\text{Im}_2]$ (5)	50	$a = 26.9 \text{ \AA}$ $b = 128.2 \text{ \AA}$	0.0729/0.018	(20)
			0.0156/1	(02)
			0.038/0.750	(11)
			0.047/0.594	(06)
$[\text{PdImCl}(\text{CNC}_6\text{H}_4(\text{OC}_{12}\text{H}_{25})_3)]$ (9)	45	$a = 30.4 \text{ \AA}$ $b = 48.7 \text{ \AA}$ $\beta = 66.2^\circ$	0.0224/0.969	(01)
			0.0338/1	(11)
			0.0494/0.500	(11)
				(11)

^aCompounds 2–5 present a centered rectangular unit cell (Col_r), whereas compound 9 shows a columnar oblique structure (Col_{ob}). The cell parameters depend weakly on the temperature.

The procedure is based on the inverse Fourier transform of the diffraction diagram. Briefly, the intensity of a given (hl) reflection is proportional to the square modulus of the complex (hl) Fourier component of the periodic electron density of the structure. Accordingly, apart from the peak angular positions, the intensity of the different reflections must also be considered. The technical details of the procedure to obtain the charge-density map can be found in ref 18. It is worth noting that the method has some ambiguity, because the phases of the different Fourier components are not experimentally accessible. As a consequence, more than one map can be compatible with the X-ray pattern of a compound. However, as in the present case, this ambiguity is easily worked out in simple cases with a few reflections. For example, only four essentially different maps result in the worst case for the materials under investigation. The choice of the correct electron charge distribution is made according to packing conditions, molecular sizes, and optimization of the steric interactions.

In the case of dinuclear palladium complexes, we considered the simplest case of a rectangular centered structure. Accordingly, we indexed the diffraction diagrams as indicated in Table 2.

The dinuclear palladium complexes (compounds 2–5) present similar charge-density maps. As an example, Figure 2a shows the X-ray scattering pattern for compound 2. In Figure 2b the small-angle region is detailed and the proposed indexation scheme is presented. The corresponding electron density distribution is shown in Figure 2c. In the figure the molecule has been drawn on the left-hand side at the same scale. The highest density areas (the brightest ones) correspond to the palladium fragments, since these groups are expected to concentrate the most important charge density. The two secondary maxima in the unit cell can be attributed to the triphenylene groups that also present a remarkable charge density. As can be seen, the molecular length between the palladium fragments and the triphenylene groups (23 Å, calculated with ACD Laboratories ChemsSketch) matches the

corresponding distances in the charge-density map. We can therefore conclude that the proposed solution gives rise to a reasonable structural model for compounds 2–5.

Additionally, the mass density of the different compounds has been measured. In the case of the dinuclear palladium complexes it is about 1.2 g/cm³ for all of the compounds. This fact implies that four molecules per unit cell must be accommodated within an average distance of about 5.5 Å in the direction parallel to the column axis. A proposed arrangement for one pair of molecules is presented in Figure 2c. As can be seen, the triphenylene groups appear superimposed whereas the palladium fragments are arranged in parallel in the plane of the figure, because their large thickness (about 5–6 Å) is not compatible with their superposition along the columnar axis.

A similar study was also carried out for compound 9. In this case the X-ray diffraction pattern was indexed on the basis of an oblique lattice. In Figure 3a the X-ray pattern is depicted. The small-angle region with the indexation scheme is shown in Figure 3b. The electron density distribution proposed for this compound appears in Figure 3c with the corresponding comparison to the molecular structure. In this case two regions of high charge density can be observed per unit cell. These maxima correspond to the palladium fragments (the highest) and to the triphenylene groups, respectively. A good agreement between the corresponding molecular length and the distance between charge density maxima is observed as well. The density mass is in this case 1.08 g/cm³, which implies, as in the previous example, that two molecules per unit cell must be placed within a distance of 5.4 Å along the column. Therefore, the two triphenylene groups can be superimposed to accommodate two thicker palladium fragments in the plane of the figure. The proposed structure appears sketched in Figure 3c and features a polymer-like arrangement of columns alternating stacking of triphenylenes with stacking of two ortho-palladated dimeric moieties.

Photophysical Studies. The UV–vis absorption and fluorescence spectra of the free imine and the palladium

complexes in dichloromethane solution are all summarized in Table 3.

Table 3. UV–Visible and Luminescence Data for the Free Imine and for Their Ortho-Palladated Complexes in Dichloromethane Solution at 298 K (10^{-5} M)

compound	λ/nm ($\epsilon/\text{mol}^{-1}\text{cm}^{-1}$)	$\lambda_{\text{ex}}/\text{nm}$	$\lambda_{\text{em}}/\text{nm}$	$10^{-3}\Phi_{\text{f}}$
ImH	344 (16414), 308 (32427), 279 (110993), 270 (73662), 261 (51844)	278	385	7.02
1	342 (30387), 307 (74714), 278 (262353), 270 (178111), 261 (128368)	267	385	4.95
2	346 (25730), 307 (68980), 279 (227063), 269 (172901), 260 (134156)	288	386	1.16
3	346 (25334), 308 (67425), 279 (230400), 270 (178237), 260 (148015)	288	385	1.24
4	347 (15608), 308 (44122), 279 (150877), 270 (107455), 260 (79840)	281	385	3.56
5	346 (32968), 308 (73805), 278 (249502), 270 (197709), 261 (158366)	285	385	1.68
6	344 (35079), 308 (78098), 279 (265253), 270 (200221), 262 (156900)	288	385	0.91
7	344 (9592), 308 (30291), 279 (119449), 269 (85321), 261 (66136)	279	385	7.85
8	345 (12656), 307 (42587), 279 (138509), 269 (102149), 261 (80052)	279	385	5.67
9	345 (13235), 308 (41696), 279 (144292), 269 (103592), 261 (78714)	279	385	5.48

The electronic spectra are all very similar, displaying a very structured spectral pattern with absorption bands and extinction coefficients typical of triphenylene chromophores (Figure 4),

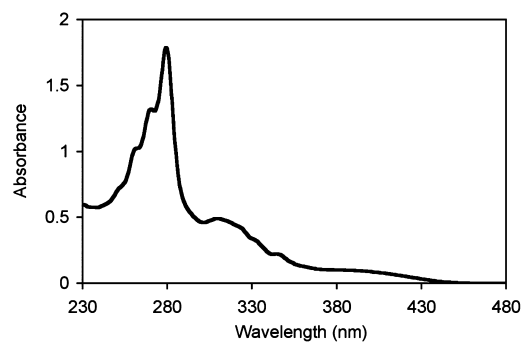


Figure 4. Absorption spectrum of $(\mu\text{-Cl})_2[\text{Pd}_2\text{Im}_2]$ (**2**), recorded in CH_2Cl_2 solution (10^{-6} M) at room temperature.

which are assigned to triphenylene $\pi\text{-}\pi^*$ transitions.¹⁹ In the complexes described here the imine group is located too far from the triphenylene core to expect any significant influence on its electronic transitions. Indeed, the imine and the palladium complexes display similar electronic spectra. It is also well-known that the presence of long chains in hexakis(*n*-alkoxy)-triphenylenes does not significantly affect the spectroscopic properties of the chromophore in solution.^{19a}

The fluorescence spectroscopic data for the free imine and the orthometalated complexes are given in Table 3. The free imine and the palladium complexes are luminescent at room temperature in dichloromethane solution. As for the electronic spectra, all of the emission spectra are similar, with a very structured pattern with the maximum at ca. 385 nm (Figure 5), typical of fluorescent 2,3,6,7,10,11-hexaalkoxytriphenylenes.^{19a} The quantum yields for the complexes, Φ_{f} , measured in dichloromethane solution at room temperature,²⁰ are smaller

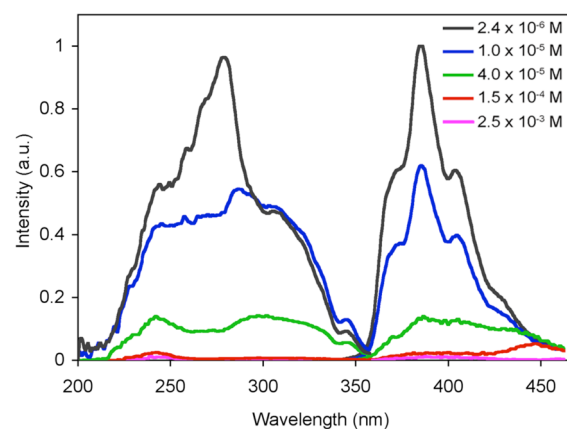


Figure 5. Normalized luminescence excitation and emission spectra of **2** in dichloromethane solution at different concentrations.

than that for 2,3,6,7,10,11-hexadodecyloxytriphenylene under the same conditions (0.17). Therefore, although the imine and the ortho-metalated fragment are not directly connected electronically, they enhance nonradiative deactivation process in these systems.

In the solid state, the luminescent behavior of these derivatives is lost. The luminescence spectra of **2** in dichloromethane solution, as a function of concentration, are shown in Figure 5. As the concentration is gradually increased from 10^{-6} to 10^{-3} M, the intensity of the emission bands decreases and the emission is lost at higher concentration. This behavior suggests the formation of nonemissive excimer or excimer-like adducts.²¹

In summary, mesomorphic mono and dinuclear ortho-palladated complexes with an unusual luminescent imine, containing a substituted triphenylene motif, have been prepared. Although the free imine ligand obtained is not mesogenic, most of the dinuclear palladium compounds, and the mononuclear trialkoxyphenyl isocyanide complex, give rise to mesophases with very interesting columnar arrangements. The discoid triphenylene moieties, having a strong tendency to stack as columns, force the metal-containing moieties to also stack in columnar zones. Due to the greater thickness of the latter, they arrange themselves in pairs of two parallel dimeric Pd cores, so as to better match the thickness of two stacked disks of triphenylene. Thus, in the LC structure the columnar Pd zones are flanked by two columns of triphenylenes, keeping the triphenylene/Pd = 1/1 ratio. In contrast, in the monomeric complex, where the Pd atom bears a discoid isocyanide ligand attached to it, a polymer-like structure is adopted in which the triphenylene and the Pd-containing zones alternate, again keeping the triphenylene/Pd = 1/1 ratio. This original accumulation, in a fluid material, of Pd-containing columnar zones supported by fully organic columns, although not associated with Pd–Pd bonds at the moment, merits further investigation and elaboration.

■ ASSOCIATED CONTENT

📄 Supporting Information

Text and figures giving full details of the synthetic methods together with the spectroscopic and analytical data for the prepared compounds, DSC scans, X-ray diffractograms, and POM textures. This material is available free of charge via the Internet at <http://pubs.acs.org>.

■ AUTHOR INFORMATION

Corresponding Authors

*E-mail for P.E.: espinet@qi.uva.es.

*E-mail for S.C.: scoco@qi.uva.es.

Notes

The authors declare no competing financial interest.

■ ACKNOWLEDGMENTS

This work was sponsored by the Ministerio de Ciencia e Innovación (Project CTQ2011-25137), the Junta de Castilla y León (Project VA302U13), MICINN-FEDER of Spain-UE (Project MAT2012-38538-C03-02), and the Basque Country Government (Project GI/IT-449-10). E.T. and G.S.-E. thank the European Commission (Erasmus Mundus) and the Basque Country University, respectively, for grants. The authors thank one of the reviewers for helpful suggestions about the structural characterization of the mesophases and Prof. Jesús Etxebarria (Basque Country University) for valuable discussions on the paper.

■ REFERENCES

- (1) (a) Kaafarani, B. R. *Chem. Mater.* **2011**, 378–396. (b) Pisula, W.; Zorn, M.; Chang, J. C.; Müllen, K.; Zentel, R. *Macromol. Rapid Commun.* **2009**, 30, 1179–1202. (c) Kato, T.; Yasuda, T.; Kamikawa, Y. *Chem. Commun.* **2009**, 729–739. (d) Sergeev, S.; Pisula, W.; Geerts, Y. H. *Chem. Soc. Rev.* **2007**, 36, 1902–1929. (e) Laschat, S.; Baro, A.; Steinke, N.; Giesselmann, F.; Hägele, C.; Scalia, G.; Judele, R.; Kapatsina, E.; Sauer, S.; Schreivogel, A.; Tosoni, M. *Angew. Chem., Int. Ed.* **2007**, 46, 4832–4887.
- (2) (a) Hains, A. W.; Liang, Z.; Woodhouse, M. A.; Gregg, B. A. *Chem. Rev.* **2010**, 110, 6689–6735. (b) Oukachmih, M.; Destruel, P.; Seguy, L.; Ablart, G.; Jolinat, P.; Archambeau, S.; Mabilia, M.; Fouet, S.; Bock, H. *Sol. Energy Mater. Sol. Cells* **2005**, 85, 535–543. (c) Schmidt-Mende, L.; Fechtenkötter, A.; Mullen, K.; Moons, E.; Friend, R.; MacKenzie, J. *Science* **2001**, 293, 1119–1122.
- (3) (a) Shimizu, Y.; Kurobe, A.; Monobe, H.; Terasawa, N.; Kiyohara, K.; Uchida, K. *Chem. Commun.* **2003**, 1676–1677. (b) Bushby, R. J.; Boden, N.; Kilner, C. A.; Lozman, O. R.; Lu, Z.; Liu, Q.; Thornton-Pett, M. A. *J. Mater. Chem.* **2003**, 13, 470–474. (c) Kato, T.; Mizoshita, N.; Kishimoto, K. *Angew. Chem., Int. Ed.* **2006**, 45, 38–68. (d) Kumar, S. *Chem. Soc. Rev.* **2006**, 35, 83–109. (e) Kumar, S. *Liq. Cryst.* **2005**, 32, 1089–1113. (f) Kumar, S. *Liq. Cryst.* **2004**, 31, 1037–1059. (g) Gupta, S. K.; Raghunathan, V.; Kumar, S. *New J. Chem.* **2008**, 33, 112–117. (h) Bisoyi, H. K.; Kumar, S. *Tetrahedron Lett.* **2008**, 49, 3628–3631. (i) Feng, X.; Marcon, V.; Pisula, W.; Hansen, M. R.; Kirkpatrick, J.; Grozema, F.; Andrienko, D.; Kremer, K.; Müllen, K. *Nat. Mater.* **2009**, 8, 421–426. (j) Tahar-Djebbar, I.; Nekelson, F.; Heinrich, B.; Donnio, B.; Guillon, D.; Kreher, D.; Mathevet, F.; Attias, A.-J. *Chem. Mater.* **2011**, 23, 4653–4656. (k) Sauer, S.; Steinke, N.; Baro, A.; Laschat, S.; Giesselmann, F.; Kantelechner, W. *Chem. Mater.* **2008**, 20, 1909–1915.
- (4) (a) Espinet, P.; Esteruelas, M. A.; Oro, L.; Serrano, J. L.; Sola, E. *Coord. Chem. Rev.* **1992**, 117, 215–274. (b) *Metallomesogens*; Serrano, J. L., Ed.; VCH: Weinheim, Germany, 1996. (c) Donnio, B.; Guillon, D.; Bruce, D. W.; Deschenaux, R. *Metallomesogens*. In *Comprehensive Organometallic Chemistry III: From Fundamentals to Applications*; Crabtree, R. H.; Mingos, D. M. P., Eds.; Elsevier: Oxford, U.K., 2006; Vol. 12 (Applications III: Functional Materials, Environmental and Biological Applications), Chapter 12.05, pp 195–294. (d) Donnio, B. *Inorg. Chim. Acta* **2014**, 409, 53–67.
- (5) Bruce, D. W. In *Inorganic Materials*, 2nd ed.; Bruce, D. W.; O'Hare, D., Eds.; Wiley: Chichester, U.K. 1996; Chapter 8.
- (6) (a) Coco, S.; Cordovilla, C.; Domínguez, C.; Donnio, B.; Espinet, P.; Guillon, D. *Chem. Mater.* **2009**, 21, 3282–3289. (b) Domínguez, C.; Heinrich, B.; Donnio, B.; Coco, S.; Espinet, P. *Chem. Eur. J.* **2013**, 19, 5988–5995.
- (7) (a) Kreuder, W.; Ringsdorf, H.; Hermann-Schönherr, O.; Wendorff, J. H. *Angew. Chem., Int. Ed. Engl.* **1987**, 26, 1249–1252. (b) Mahlstedt, S.; Janietz, D.; Strake, A.; Wendorff, J. H. *Chem. Commun.* **2000**, 15–16. (c) Kouwer, P. H. J.; Pourzand, J.; Mehl, G. H. *Chem. Commun.* **2004**, 66–67. (d) Kouwer, P. H. J.; Mehl, G. H. *J. Mater. Chem.* **2009**, 19, 1564–1575. (e) Tanaka, D.; Ishiguru, H.; Shimizu, Y.; Uchida, K. *J. Mater. Chem.* **2012**, 22, 25065–25071.
- (8) Kumar, S.; Varshney, S. K. *Liq. Cryst.* **2001**, 28, 161–163.
- (9) Schulte, J. L.; Laschat, S.; Schulte-Ladbeck, R.; von Arnim, V.; Schneider, A.; Finkelmann, H. *J. Organomet. Chem.* **1998**, 552, 171–176.
- (10) Cammidge, A. N.; Gopee, H. *Chem. Commun.* **2002**, 966–967.
- (11) Mohr, B.; Wegner, G.; Ohta, K. *Chem. Commun.* **1995**, 995–996.
- (12) Yang, F.; Bai, X.; Guo, H.; Li, C. *Tetrahedron Lett.* **2013**, 54, 409–413.
- (13) (a) Ros, M. B.; Ruiz, N.; Serrano, J. L.; Espinet, P. *Liq. Cryst.* **1991**, 9, 77–96. (b) Coco, S.; Cordovilla, C.; Espinet, P.; Gallani, J.-L.; Guillon, D.; Donnio, B. *Eur. J. Inorg. Chem.* **2008**, 1210–1218.
- (14) Kumar, S.; Manickam, M. *Synthesis* **1998**, 1119–1122.
- (15) Baena, M. J.; Espinet, P.; Ros, M. B.; Serrano, J. L. *J. Mater. Chem.* **1996**, 6, 1291–1296.
- (16) (a) Onoue, H.; Minami, K.; Nakagawa, K. *Bull. Chem. Soc. Jpn.* **1970**, 43, 3480–3485. (b) Nakamoto, N. *IR and Raman Spectra of Inorganic and Coordination Compounds*, 3rd ed.; Wiley-Interscience: New York, 1978. (c) Baena, M. J.; Buey, J.; Espinet, P.; Kitzerow, H.-S.; Heppke, G. *Angew. Chem., Int. Ed.* **1993**, 32, 1201–1203. (d) Baena, M. J.; Buey, J.; Espinet, P.; García-Prieto, C. E. *J. Organomet. Chem.* **2005**, 690, 998–1010.
- (17) Buey, J.; Diez, G. A.; Espinet, P.; García-Granda, S.; Pérez-Carreño, E. *Eur. J. Inorg. Chem.* **1998**, 9, 1235–1241.
- (18) Folcia, C. L.; Alonso, I.; Ortega, J.; Etxebarria, J.; Pintre, I.; Ros, M. B. *Chem. Mater.* **2006**, 18, 4617–4626.
- (19) (a) Markovitsi, D.; Germain, A.; Millié, P.; Lécuyer, P.; Gallos, L. K.; Argyrakis, P.; Bengs, H.; Ringsdorf, H. *J. Phys. Chem.* **1995**, 99, 1005–1017. (b) Marguet, S.; Markovitsi, D.; Millié, P.; Sigal, H.; Kumar, S. *J. Phys. Chem. B* **1998**, 102, 4697–4710.
- (20) Velapoldi, R. A.; Tønnesen, H. H. *J. Fluoresc.* **2004**, 14, 465–472.
- (21) (a) Turro, N. J. *Modern Molecular Photochemistry*; University Science Books: Mill Valley, CA, 1991. (b) Birks, J. B. *Photophysics of Aromatic Molecules*; Wiley-Interscience: New York, 1970.